Report

Current Biology

Cell-Specific Transcriptional Profiling of Ciliated Sensory Neurons Reveals Regulators of Behavior and Extracellular Vesicle Biogenesis

Highlights

- Extracellular vesicle (EV)-releasing neuron (EVN) genes act in sensory signaling
- This is the first cell-specific profile of EVNs isolated from adult *C. elegans*
- TRAF homologs are required for polycystin-mediated male mating behaviors
- p38 MAPK PMK-1 regulates EV biogenesis independent of its canonical kinase cascade

Authors

Juan Wang, Rachel Kaletsky, Malan Silva, ..., David H. Hall, Coleen T. Murphy, Maureen M. Barr

Correspondence

barr@dls.rutgers.edu

In Brief

Cilia and extracellular vesicles (EVs) are physically associated from alga to man, suggesting ancient function. Wang et al. isolated and profiled ciliated EV-releasing neurons from adult *C. elegans* and identified 335 signature genes. These studies provide insight into the fundamental biology of EVs and the intimate relationship between EVs and cilia.

Wang et al., 2015, Current Biology *25*, 3232–3238
December 21, 2015
http://dx.doi.org/10.1016/j.cub.2015.10.057

CellPress

CellPress

Current Biology
Report

Cell-Specific Transcriptional Profiling of Ciliated Sensory Neurons Reveals Regulators of Behavior and Extracellular Vesicle Biogenesis

Juan Wang,[1] Rachel Kaletsky,[2] Malan Silva,[1] April Williams,[2] Leonard A. Haas,[1] Rebecca J. Androwski,[1] Jessica N. Landis,[2] Cory Patrick,[1] Alina Rashid,[1] Dianaliz Santiago-Martinez,[1] Maria Gravato-Nobre,[3] Jonathan Hodgkin,[3] David H. Hall,[4] Coleen T. Murphy,[2] and Maureen M. Barr[1,*]

[1]Department of Genetics and Human Genetics Institute, Rutgers University, Piscataway, NJ 08854, USA
[2]Department of Molecular Biology and Lewis Sigler Institute, Princeton University, Princeton, NJ 08544, USA
[3]Department of Biochemistry, University of Oxford, Oxford OX1 3QU, UK
[4]Center for *C. elegans* Anatomy, Albert Einstein College of Medicine, 1410 Pelham Parkway, Bronx, NY 10461, USA
*Correspondence: barr@dls.rutgers.edu
http://dx.doi.org/10.1016/j.cub.2015.10.057

SUMMARY

Cilia and extracellular vesicles (EVs) are signaling organelles [1]. Cilia act as cellular sensory antennae, with defects resulting in human ciliopathies. Cilia both release and bind to EVs [1]. EVs are submicron-sized particles released by cells and function in both short- and long-range intercellular communication. In *C. elegans* and mammals, the autosomal dominant polycystic kidney disease (ADPKD) gene products polycystin-1 and polycystin-2 localize to both cilia and EVs, act in the same genetic pathway, and function in a sensory capacity, suggesting ancient conservation [2]. A fundamental understanding of EV biology and the relationship between the polycystins, cilia, and EVs is lacking. To define properties of a ciliated EV-releasing cell, we performed RNA-seq on 27 GFP-labeled EV-releasing neurons (EVNs) isolated from adult *C. elegans*. We identified 335 significantly overrepresented genes, of which 61 were validated by GFP reporters. The EVN transcriptional profile uncovered new pathways controlling EV biogenesis and polycystin signaling and also identified EV cargo, which included an antimicrobial peptide and ASIC channel. Tumor-necrosis-associated factor (TRAF) homologs *trf-1* and *trf-2* and the p38 mitogen-activated protein kinase (MAPK) *pmk-1* acted in polycystin-signaling pathways controlling male mating behaviors. *pmk-1* was also required for EV biogenesis, independent of the innate immunity MAPK signaling cascade. This first high-resolution transcriptome profile of a subtype of ciliated sensory neurons isolated from adult animals reveals the functional components of an EVN.

RESULTS AND DISCUSSION

The cilium both releases and binds to extracellular vesicles (EVs), suggesting that cilia may be essential in EV-mediated communication as both senders and receivers of information [3–8]. EVs carry specific protein and RNA cargoes that can be transferred between donor and recipient cells without requiring direct contact [9]. EVs mediate a broad range of physiological and pathological processes [10].

The mammalian polycystins localize to cilia as well as urinary EVs released from renal epithelial cells [3, 11–13], and polycystin ciliary trafficking defects may be an underlying cause of autosomal dominant polycystic kidney disease (ADPKD) [14]. In an amazing display of evolutionary conservation, we recently showed that the *C. elegans* cilium is a source of bioactive polycystin-containing EVs [6]. The mechanisms controlling EV biogenesis, shedding, and release are poorly understood, largely due to technical difficulties in visualizing, isolating, and characterizing these sub-micrometer-sized particles. Here, we defined the unique features of a ciliated EV-releasing neuron (EVN).

C. elegans shed and release EVs from 27 ciliated EVNs including six inner labial type 2 (IL2) neurons and 21 male-specific polycystin-expressing EVNs in the head (four CEM neurons) and tail (16 ray B-type RnB neurons and one hook B-type HOB neuron; Figures 1A and 1B) [6]. In these male-specific EVNs, the polycystins *lov-1* and *pkd-2* are required for male sex drive, response to mate contact, and vulva location [15–17]. The kinesin-3 protein KLP-6 is exclusively expressed in the 27 EVNs and is required for release of bioactive PKD-2::GFP-containing EVs that function in reproductive animal-to-animal communication [6]. Intact cilia, but not multivesicular body components, are required for EV release, suggesting that PKD-2-containing EVs are not exosomes but rather ectosomes that bud from the plasma membrane at the ciliary base [6]. In addition to *klp-6* and the polycystins, only a handful of genes (coexpressed with polycystin genes *cwp-1* to *-5*, alpha-tubulin *tba-6*, and the EV release regulator *cil-7*) are exclusively expressed in the EVNs [18–21].

To decipher the biology of a polycystin-expressing EVN in its native environment, we isolated *klp-6p*::GFP-labeled neurons from age-synchronized adult animals by mechanical and proteolytic disruption, filtration, and FACS [22] (Figure 1C). Animals were alive until the moment they were processed. Therefore, samples are as close to the in vivo state as one can get (as opposed to the re-differentiated and fixed cells that other labs have used), which makes profiling results more biologically

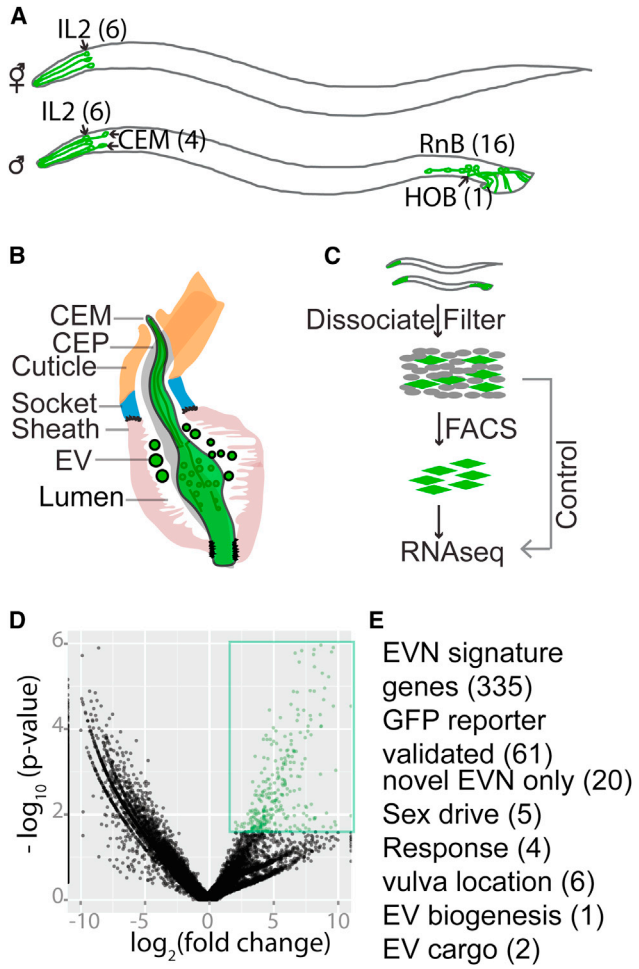

Figure 1. Cell-Type RNA-Seq to Define the EVN Transcriptome

(A) The ciliated EVNs, six in the hermaphrodite (top) and 27 in male (bottom).

(B) The male cephalic sensillum. Glial sheath and socket cells form a continuous lumen surrounding the CEM neuronal cilium, which is exposed to the environment directly through a cuticular opening. The lumen is shared by CEM and CEP neurons. EVs are observed in the lumen.

(C) Schematic illustration of the differential RNA-seq experiment. EVNs were FACS purified from dissociated and filtered cells isolated from synchronized *klp-6p*::GFP expressing young adult males and hermaphrodites, followed by mRNA extraction, library construction, and RNA-seq. Refer to Figure S1 for heatmap, principal-component analysis, and downsampling in silico.

(D) Volcano plot showing 335 genes differentially overrepresented in sorted EVNs (colored and boxed in green) compared to whole worms at a false discovery rate of 10%.

(E) 335 EVN gene signature genes were validated by GFP expression pattern and functional analysis (for available mutants).

The number of genes for each category is listed in parentheses. Refer to Tables S1 and S2 for full list of 335 signature genes and original DEseq data, respectively. See Table S3 for GO analysis of EVN overrepresented genes.

accurate. RNA from two replicates (8,000 and 11,000 EVNs) was purified and amplified for RNA-seq (Experimental Procedures). RNA-seq libraries from the amplification products of EVN cell populations and whole-worm lysate control samples were sequenced. Total reads were downsampled in silico to a depth of 4.2–6.7 × 10^6 reads per library and tested for expression and differential expression (Figures S1C and S1D). DEseq software identified 9,922 genes expressed in EVNs, 14,455 genes in whole worm (Table S2), and 335 genes significantly overrepresented 2- to 11-fold in EVNs (Figure 1D; Table S1). Cluster analysis of the total 14,455 genes expressed between sorted EVNs and whole worm showed high intragroup homogeneity (Figure S1A). Principal-component analysis showed clear separation between sorted EVNs and whole worm lysates (Figure S1B). Volcano plot of the differential RNA-seq transcriptome analysis showed close linearization of log2 fold change and the log 10 p value, indicating most data points were consistently represented in both replicates (Figure 1D).

To uncover the functions of the 335 overrepresented genes, we used gene ontology (GO) term annotation analysis. Among the GO terms in the 335 overrepresented genes were neuropeptide signaling, ciliogenesis, neuron projection, ion channel activity, and synaptic transmission, which are consistent with the neuronal and ciliated characters of the EVNs (Table S3). Over half of the overrepresented genes including 70 in the top 100 have no assigned name or described RNAi phenotype, likely because global RNAi screens do not examine adult male phenotypes. Thus, many of these EVN signature genes may function specifically in the adult male. Sixty-one of 335 signature genes were expressed in EVNs as demonstrated by published GFP expression analysis or described herein (Table S1). The EVN-restricted genes *klp-6*, *lov-1*, *pkd-2*, *cil-7*, and the five *cwp* genes [16, 18–20, 23] were upregulated 5.8-fold or higher. We identified 20 new genes that were exclusively expressed in all EVNs, similar to the EVN release regulators *klp-6* and *cil-7* (Figure 2A); in all male-specific EVNs, similar to *pkd-2* and *lov-1* (Figure 2B); or in a subset of the EVNs (Figures 2C and 2D), including Y70G10A.2 that was expressed in a single EVN (Figure 2D). Combined, these results indicate that our RNA-seq data set is reliable and highly enriched for EVN genes and demonstrate the sensitivity of our profiling method.

TNF receptor-associated factors (TRAFs) act as signaling adaptors for the TNFR superfamily, Toll-like receptor, and many other receptors [24]. We found that the *C. elegans* TRAF homologs *trf-1* and *trf-2* were overrepresented 8.6-fold in EVNs (Table S1) and exclusively expressed in the male-specific EVNs (Figures 3A–3D). TRF-1 is a canonical TRAF, with a RING domain, a TRAF zinc finger domain, and a MATH (meprin-associated TRAF homology) domain, whereas *trf-2* (Y110A7A.2) encodes a MATH-domain-only protein (Figures 3A and 3C). GFP-tagged TRF-1 and TRF-2 localized throughout male-specific EVNs including cilia, dendrites, cell bodies, and axons but were excluded from nuclei (Figures 3B and 3D). We did not observe TRF-1::GFP or TRF-2::GFP released in the extracellular environment, indicating that, unlike the polycystins LOV-1 and PKD-2, TRF-1 and TRF-2 are not EV cargo.

trf-1 and *trf-2* were required for all polycystin-mediated male behaviors: sex drive; response; and vulva location (Figures 3E, 3F, and 4G). Neither *trf-1* nor *trf-2* was required for PKD-2::GFP localization to cilia or EVs or for ciliogenesis in EVNs. The *trf-2*; *trf-1* double mutant was not more response or location of vulva (Lov) defective than the *trf-1* single mutant, indicating that *trf-1* and *trf-2* act non-redundantly. The *lov-1*; *pkd-2*; *trf-1* triple mutant and *lov-1*; *trf-1* and *trf-1*; *pkd-2* doubles were indistinguishable from each other, indicating that polycystins and TRAFs act in the same genetic pathway (Figure 3F). *tol-1* (the

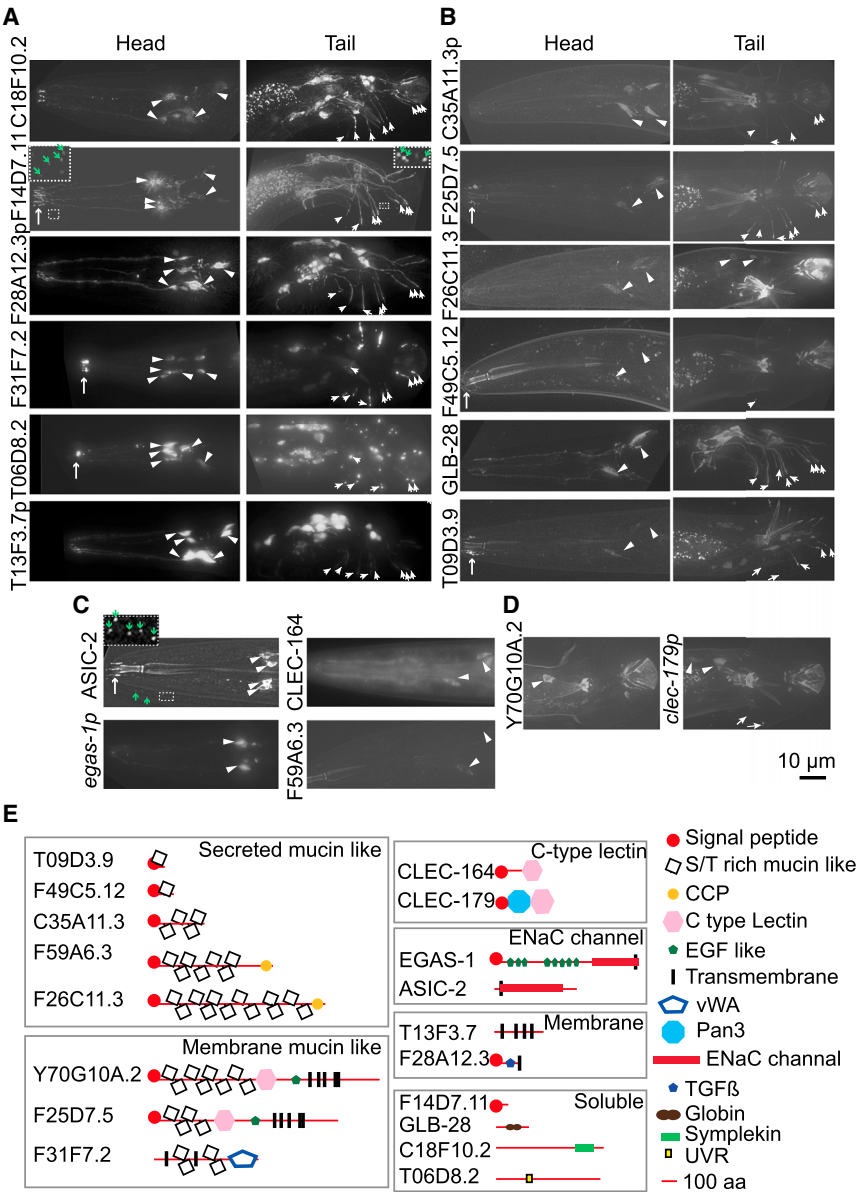

Figure 2. EVN Signature Genes Were Expressed in All 27 EVNs, the 21 Polycystin-Expressing EVNs, or a Subset Thereof

(A) Head IL2 and CEM (left) and tail HOB and RnB (right) images of GFP reporters that were expressed exclusively in all 27 EVNs.

(B) A subset of EVN signature genes showed expression in only the male-specific head CEM (left) and tail HOB and RnB (right) neurons. In (A) and (B), arrowheads point to cell bodies in the head and to ray dendrites in the tail. The scale bar represents 10 µm.

(C) *asic-2* was expressed in the six IL2 neurons, *egas-1* in four IL2 quadrant (IL2Q) neurons, and *clec-164* and F59A6.3 in CEM neurons.

(D) Y70G10A.2 was expressed only in the HOB EVN and *clec-179* in HOB and a few ray EVNs. In all panels, translational GFP reporters are shown by gene name or open reading frame number and transcriptional (promoter) GFP reporters are shown by gene name or ORF followed by *p*. For translational reporters, arrows point to ciliary localization. In (A) and (C), dashed line boxes were 4× scaled with enhanced contrast and brightness to visualize EVs (green arrows). F14D7.11::GFP localized in cilia and secreted EVs from all 27 EVNs and ASIC-2::GFP localized in IL2 cilia and secreted EVs.

(E) Domain analysis of validated genes. Signal peptide sequences were predicted by SignalP 4.1 Server (http://www.cbs.dtu.dk/services/SignalP/). Mucin-domain-containing proteins are predicted to be secreted and extensively O-glycosylated in the serine (S)- or threonine (T)-rich domain. Transmembrane domains were predicted by the TM Pred server (http://www.ch.embnet.org/software/TMPRED_form.html). CCP, C-type lectin (CLEC), Pan3, TGFβ, EGF-like, DEG/ENaC channel, vWA (Von Willebrand factor type A), globin, and UVR domains were predicted by Wormbase.

Refer to Table S4 for a listing of EVN signature genes with predicted or demonstrated function in stress response or innate immunity.

sole Toll-like receptor in *C. elegans*) and *ikb-1* (inhibitor of kappa beta homolog) were not overrepresented in EVNs and were not required for response or vulva location (Figure 3E). These data indicate that the *C. elegans* TRAFs, but not other components of the Toll pathway, act in polycystin-mediated sensory signaling.

In addition to the TRAFs, a significant number of EVN signature genes were implicated in cellular stress or innate immune responses (Table S4). The stress-activated p38 mitogen-activated protein kinase (MAPK) homolog *pmk-1* was overrepresented in EVNs. *pmk-1* mutant males were defective in EV biogenesis and release (Figures 4A–4E). 100% of wild-type late L4 larval and adult males released PKD-2::GFP-containing EVs from the ciliated sensory neurons in the head (CEMs) and tail (RnBs and HOB; Figures 4A and 4B). In contrast, less than 10% of L4 *pmk-1* and 50% of adult *pmk-1* mutant males released PKD-2::GFP-labeled EVs (Figure 4B). Ciliary localization of PKD-2::GFP appeared similar between wild-type and *pmk-1* males (Figure 4A). We conclude that *pmk-1* regulates release of PKD-2::GFP-containing EVs, but not ciliary localization of PKD-2::GFP.

To examine *pmk-1* ciliary and EV ultrastructure, we used serial thin-cut transmission electron microscopy. In the wild-type cephalic sensillum, EVs are found in the lumen formed by glial-like support cells and surrounding the CEM and CEP cilia [6] (Figures 4C and 4D). In the *pmk-1* cephalic sensillum, EVs were largely absent from the lumen and CEM cilia had fewer doublets than the expected nine (Figure 4C). The quantity of lumen EVs in *pmk-1* mutant males was significantly reduced, indicating an EV biogenesis defect (Figures 4D and 4E). *pmk-1* mutant males were also response and Lov defective but displayed normal sex drive (Figure 4F). Similarly, the EV release regulators *klp-6*

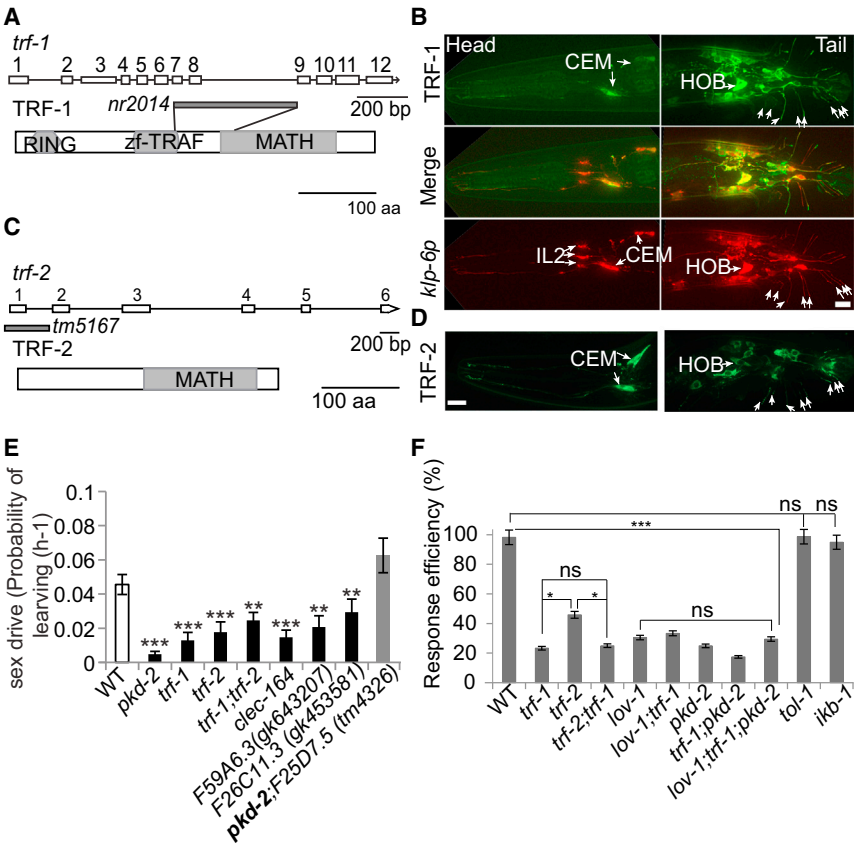

Figure 3. *trf-1* and *trf-2* Coexpressed in Male-Specific EVNs and Acted in the Polycystin-Signaling Pathways

(A and C) Schematic of *trf-1* and *trf-2* genomic and protein structure, with molecular lesions indicated in genomic structure.

(A) The *trf-1* locus encodes all common domains shared by mammalian TRAFs: a RING finger domain that may act as an E3 ubiquitin-ligase and a TRAF zinc finger and MATH domain that may mediate protein-protein interaction or oligomerization. The *trf-1(nr2041)* mutation deletes part of the zf-TRAF domain and part of the MATH domain and may affect mRNA splicing.

(B) *trf-1* was co-expressed with *klp-6* in male-specific, but not IL2, EVNs.

(C) TRF-2 has only a MATH domain. The *trf-2(tm5167)* deletion removes upstream of first exon to the end of the first intron.

(D) TRF-2::GFP was expressed and localized in the same pattern as TRF-1::GFP.

(E) TRAF, lectins, and adhesion molecules were required for male sex drive. The *tm4326* deletion allele of F25D7.5 suppresses the sex drive defect of *pkd-2* mutant males (in bold). The probability of the male leaving the food lawn per hour PL(h-1) is indicated on the y axis, the male's genotype on the x axis. Data were analyzed by Kruskal-Wallis test. *p < 0.05; **p < 0.01; ***p < 0.001.

(F) Response efficiency (RE) of *lov-1*, *pkd-2*, *trf-1*, *trf-2*, and Toll pathway genes *tol-1* and *ikb-1*. Data were analyzed with Fisher's exact test, Bonferroni-Holm corrected. *p < 0.05; ***p < 0.001. ns, not significant. The minimum number (n) of individual males analyzed per genotype was 37 for sex drive and 59 for response behavior.

and *cil-7* are required for response and vulva location behaviors, but not sex drive [20]. For the EVN-specific genes regulating mating behaviors, response and vulva location depended on EV biogenesis or cilia-EV interactions, whereas sex drive was independent. These results also suggest that polycystin-mediated behaviors involve different signaling networks (Figure 4G).

In the innate immune response, *pmk-1* is the most-downstream component in a MAP kinase cascade pathway [25]. However, expression of only *pmk-1*, but not the upstream kinase cascade genes *tir-1*, *nsy-1*, and *sek-1*, was overrepresented in EVNs. We examined *tir-1*, *nsy-1*, and *sek-1* mutant males for mating behaviors and release of PKD-2::GFP-containing EVs and observed no defects (Table S4), indicating that *pmk-1* acts via an unknown EV biogenesis pathway. In cultured mammalian cells, p38 MAPK is implicated in the production of EVs from macrophages after exposure to tobacco smoke, from aortic endothelial cells induced by TNF-α, and from glial cells [26–28]. We conclude that *pmk-1* is a conserved regulator of EV biogenesis that acts independent of the innate immune MAPK cascade. These data also reveal the potential of EVN signature gene data set to uncover new pathways in EV biology.

Our EVN profile identified many transmembrane (TM) proteins (Table S1 with annotation of signal peptide + TM domain-containing proteins) and several channels (Figure 2E; Table S1), including two acid-sensing/amiloride-sensitive ion channels (ASICs). *asic-2* and *egas-1* are expressed in the shared IL2 neurons (Figure 2C). Neither *asic-2* nor *egas-1* was required for remodeling of IL2 neurons in the reproductively arrested dauer state [29] or for male mating behaviors (Table S5). ASIC-2::GFP localized to IL2 cilia and EVs secreted from IL2 neurons in reproductively growing animals. Hence, our EVN profile also identified EV cargo, including the known (LOV-1, PKD-2, CWP-1, and CIL-7) [6, 20] and new cargoes.

GFP-tagged F14D7.11 was also EV cargo, found in cilia and EVs released from all 27 EVNs (Figure 2A), similar to the EV biogenesis regulator CIL-7 [20]. F14D7.11 resembles an antimicrobial peptide (AMP) and contains a CYSTM (cysteine-rich TM) module proposed to play a role in stress tolerance [30]. Our EVN profile identified 13 AMPs, with F14D7.11 being the most highly overrepresented (Tables S1 and S4). Intriguingly, human urinary exosomes contain AMPs that have bactericidal activity [31]. An intriguing possibility is that EVs possess antimicrobial activity and play protective roles during the mating process. Alternatively, *C. elegans* could release EVs that have deleterious effects on other organisms. Consistent with this idea, unidentified *C. elegans* male secretions reduce hermaphrodite lifespan [32] and parasitic nematodes use EVs to transfer small RNAs to mammalian cells and modulate host innate immunity [33].

Several EVN signature genes encode lectins or adhesion molecules (Figure 2E; Table S4). In our data set, 13 *clec* genes were significantly overrepresented and do not overlap with those up-regulated upon infection or expressed at higher levels in the

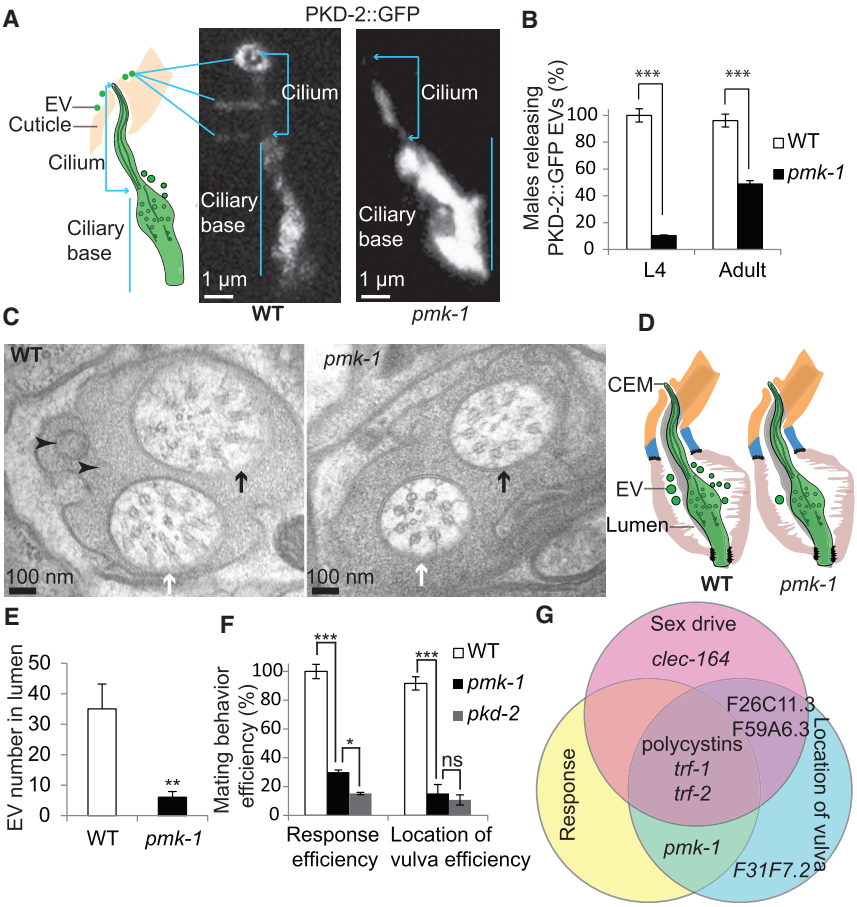

Figure 4. The *p38* MAPK *pmk-1* Was Required for EV Biogenesis and Polycystin-Mediated Response and Vulva Location Behaviors

(A) PKD-2::GFP CEM ciliary localization in wild-type and *pmk-1* males. Cartoon shows the CEM cilium protruding from the cuticular pore and EVs surrounding the cuticle. In wild-type, PKD-2::GFP localized to the ciliary base, cilium, and EVs released outside the male's nose. Note, in wild-type, EVs accumulated and surrounded the ciliary pore and cuticle. In *pmk-1* males, PKD-2::GFP localized normally to the ciliary base and cilium but was absent from EVs. To show the full length of PKD-2::GFP-labeled cilia and the EVs, images of wild-type and *pmk-1* males were taken with different exposure times and adjusted with different brightness and contrast. The original images were enlarged six times by the Photoshop CS5 image transformation tool. The scale bar represents 1 μm.

(B) *pmk-1* mutant males were defective in PKD-2::GFP-labeled EV release in both L4 (n = 20 for wild-type; n = 29 for *pmk-1*) and adult stage (n = 52 for wild-type and n = 43 for *pmk-1*). Data were analyzed with Fisher's exact test, Bonferroni-Holm corrected; ***p < 0.001.

(C and D) TEM and cartoon of wild-type and *pmk-1* cephalic sensillum at the level of the ciliary transition zone. In wild-type, EVs were present in the extracellular lumen. In *pmk-1* males, EVs numbers are significantly reduced in the cephalic lumen. In *pmk-1* males, the CEM axoneme contained eight rather than nine doublet microtubules of wild-type males. Black arrowheads, EVs; white arrows, CEM transition zone; black arrows, CEP transition zone. The scale bar represents 100 nm.

(E) Bar graph of number of EVs (mean ± SEM) in wild-type and *pmk-1*. Mann-Whitney test was used for statistical analysis; n = 7 cephalic sensillae for wild-type from two worms; n = 4 cephalic sensillae for *pmk-1* from one worm. **p = 0.01.

(F) *pmk-1* mutant males are response and Lov defective. Statistical analysis was done by Fisher's exact test, Bonferroni-Holm corrected for response efficiency, RE (n = 184 for wild-type, 60 for *pmk-1*, and 264 for *pkd-2*), and one-way ANOVA for location of vulva efficiency, LE (n = 20 for wild-type, 20 for *pmk-1*, and 18 for *pkd-2*). *p < 0.05; ***p < 0.001. ns, not significant.

(G) The *C. elegans* polycystins function in a multi-layered signaling network. Venn diagram showing polycystin-mediated mating behaviors are genetically separable. *lov-1*, *pkd-2*, and the TRAFs played a central role in sex drive, response, and vulva location whereas other genes act in specific behavioral pathways. Refer to Table S5 for RE and LE of mutants corresponding to new EVN signature genes and pathways.

bodies of adult males compared to hermaphrodites (Tables S1 and S4). To determine whether these lectins or adhesion molecules play a role in polycystin-mediated behaviors, we examined their expression patterns (Figures 2A–2D) and functions in sex drive, response, and vulva location for available mutants (Figures 3C and 4G). *clec-164* was specifically expressed in the four CEMs and required for male sex drive (Figures 2C and 3C). The single transmembrane protein F28A12.3 resembles an adhesion receptor with a cysteine-rich extracellular domain and was expressed in all 27 EVNs (Figures 2A and 2E), yet mutant males displayed normal mating behaviors (Table S5). F25D7.5 and its paralog Y70G10A.2 are predicted to encode a long extracellular region containing a C-type lectin fold and EGF domain, followed by five transmembrane-spanning domains (Figure 2E). F25D7.5 was expressed in 21 male-specific EVNs (Figure 2B) and may negatively regulate sex drive, as its mutation suppressed *pkd-2* sex drive, but not response or Lov defects (Figure 3E; Table S5). Y70G10A.2 was expressed exclusively in the HOB EVN (Figure 2D), but not required for HOB-mediated vulva location behavior (Table S5). F26C11.3 and F59A6.3 encode secreted mucin-like serine-threonine rich proteins that contain a complement control protein (CCP) domain at their C termini. F26C11.3 was expressed in 21 male-specific EVNs (Figure 2B) whereas F59A6.3 was only expressed in the CEMs (Figure 2C). F59A6.3 and F26C11.3 single mutants displayed decreased sex drive (Figure 3E); the latter were also Lov (Table S5). F31F7.2, a predicted two-transmembrane protein with a von Willebrand factor type A domain, was expressed in all 27 EVNs (Figure 2A) but required only for vulva location and not sex drive or response behavior (Table S5).

C. elegans EVNs, EVs, and EVN-expressed genes serve male reproductive signaling functions (Figure 4G). The polycystin-expressing, male-specific EVNs are required for sex drive, response, and vulva location. Some EVN-expressed genes (the TRAFs *trf-1* and *trf-2*) were required for all polycystin-mediated behaviors, whereas others played more specific behavioral functions (Figure 4G). For example, CEM-expressed *clec-164* was required only for sex drive and pan-EVN-expressed F31F7.2

only for vulva location. The p38 MAPK *pmk-1* was required for response and vulva location behavior, but not sex drive. Intriguingly, the known regulators of EV biogenesis: *pmk-1*, *cil-7*, and *klp-6* display this property [20], suggesting that luminal EVs may be required for the integrity of the male sensory organs mediating these behavioral functions. EVs play diabolical roles in the spread of toxic cargo in cancer, infectious diseases, and neurodegenerative disorders [10, 34]. We speculate that EVs may play a similar role in ADPKD and other ciliopathies. We conclude that *C. elegans* polycystin-mediated signaling pathways are genetically separable and that our EVN-expressed gene list identified new components and pathways regulating mating behavior as well as EV biogenesis, EV cargo sorting, and EV signaling.

SUPPLEMENTAL INFORMATION

Supplemental Information includes one figure, five tables, and Supplemental Experimental Procedures and can be found with this article online at http://dx.doi.org/10.1016/j.cub.2015.10.057.

ACKNOWLEDGMENTS

We thank WormBase; the National Bioresource Project for strains; Christina DeCoste for assistance with FACS; Ken Nguyen, Leslie Gunther, and Geoff Perumal for help with HPF-FS, embedding, and serial section protocols performed at Einstein; William Rice and Ed Eng at the New York Structural Biology Center (NYSBC) for help with electron tomography; Lillian Hunter for assistance with strain construction; members of the M.M.B. and C.T.M. labs and Rutgers *C. elegans* community for discussion and insight, more than we ever learned in school; Dr. Emily Troemel for critical reading of the manuscript; and Rutgers Genetics Department for sabbatical time and critical bridge funding. Use of the NYSBC facilities was supported by the Albert Einstein College of Medicine. Some strains were provided by the *Caenorhabditis* Genetics Center (CGC), which is funded by NIH Office of Research Infrastructure Programs (P40 OD010440). This work was funded by NIH DK059418 and DK074746 (to M.M.B.), NIH OD 010943 (to D.H.H.), and the Medical Research Council (to M.G.-N. and J.H.).

Received: August 4, 2015
Revised: October 23, 2015
Accepted: October 26, 2015
Published: December 10, 2015

REFERENCES

1. Wood, C.R., and Rosenbaum, J.L. (2015). Ciliary ectosomes: transmissions from the cell's antenna. Trends Cell Biol. *25*, 276–285.
2. O'Hagan, R., Wang, J., and Barr, M.M. (2014). Mating behavior, male sensory cilia, and polycystins in Caenorhabditis elegans. Semin. Cell Dev. Biol. *33*, 25–33.
3. Hogan, M.C., Manganelli, L., Woollard, J.R., Masyuk, A.I., Masyuk, T.V., Tammachote, R., Huang, B.Q., Leontovich, A.A., Beito, T.G., Madden, B.J., et al. (2009). Characterization of PKD protein-positive exosome-like vesicles. J. Am. Soc. Nephrol. *20*, 278–288.
4. Wood, C.R., Huang, K., Diener, D.R., and Rosenbaum, J.L. (2013). The cilium secretes bioactive ectosomes. Curr. Biol. *23*, 906–911.
5. Pampliega, O., Orhon, I., Patel, B., Sridhar, S., Díaz-Carretero, A., Beau, I., Codogno, P., Satir, B.H., Satir, P., and Cuervo, A.M. (2013). Functional interaction between autophagy and ciliogenesis. Nature *502*, 194–200.
6. Wang, J., Silva, M., Haas, L.A., Morsci, N.S., Nguyen, K.C., Hall, D.H., and Barr, M.M. (2014). C. elegans ciliated sensory neurons release extracellular vesicles that function in animal communication. Curr. Biol. *24*, 519–525.
7. Bakeberg, J.L., Tammachote, R., Woollard, J.R., Hogan, M.C., Tuan, H.F., Li, M., van Deursen, J.M., Wu, Y., Huang, B.Q., Torres, V.E., et al. (2011). Epitope-tagged Pkhd1 tracks the processing, secretion, and localization of fibrocystin. J. Am. Soc. Nephrol. *22*, 2266–2277.
8. Tanaka, Y., Okada, Y., and Hirokawa, N. (2005). FGF-induced vesicular release of Sonic hedgehog and retinoic acid in leftward nodal flow is critical for left-right determination. Nature *435*, 172–177.
9. Raposo, G., and Stoorvogel, W. (2013). Extracellular vesicles: exosomes, microvesicles, and friends. J. Cell Biol. *200*, 373–383.
10. EL Andaloussi, S., Mäger, I., Breakefield, X.O., and Wood, M.J. (2013). Extracellular vesicles: biology and emerging therapeutic opportunities. Nat. Rev. Drug Discov. *12*, 347–357.
11. Yoder, B.K., Hou, X., and Guay-Woodford, L.M. (2002). The polycystic kidney disease proteins, polycystin-1, polycystin-2, polaris, and cystin, are co-localized in renal cilia. J. Am. Soc. Nephrol. *13*, 2508–2516.
12. Pazour, G.J., San Agustin, J.T., Follit, J.A., Rosenbaum, J.L., and Witman, G.B. (2002). Polycystin-2 localizes to kidney cilia and the ciliary level is elevated in orpk mice with polycystic kidney disease. Curr. Biol. *12*, R378–R380.
13. Pisitkun, T., Shen, R.F., and Knepper, M.A. (2004). Identification and proteomic profiling of exosomes in human urine. Proc. Natl. Acad. Sci. USA *101*, 13368–13373.
14. Cai, Y., Fedeles, S.V., Dong, K., Anyatonwu, G., Onoe, T., Mitobe, M., Gao, J.D., Okuhara, D., Tian, X., Gallagher, A.R., et al. (2014). Altered trafficking and stability of polycystins underlie polycystic kidney disease. J. Clin. Invest. *124*, 5129–5144.
15. Barr, M.M., DeModena, J., Braun, D., Nguyen, C.Q., Hall, D.H., and Sternberg, P.W. (2001). The Caenorhabditis elegans autosomal dominant polycystic kidney disease gene homologs lov-1 and pkd-2 act in the same pathway. Curr. Biol. *11*, 1341–1346.
16. Barr, M.M., and Sternberg, P.W. (1999). A polycystic kidney-disease gene homologue required for male mating behaviour in C. elegans. Nature *401*, 386–389.
17. Barrios, A., Nurrish, S., and Emmons, S.W. (2008). Sensory regulation of *C. elegans* male mate-searching behaviour. Curr. Biol. *18*, 1865–1871.
18. Portman, D.S., and Emmons, S.W. (2004). Identification of C. elegans sensory ray genes using whole-genome expression profiling. Dev. Biol. *270*, 499–512.
19. Miller, R.M., and Portman, D.S. (2010). A latent capacity of the C. elegans polycystins to disrupt sensory transduction is repressed by the single-pass ciliary membrane protein CWP-5. Dis. Model. Mech. *3*, 441–450.
20. Maguire, J.E., Silva, M., Nguyen, K.C.Q., Hellen, E., Kern, A.D., Hall, D.H., and Barr, M.M. (2015). Myristoylated CIL-7 regulates ciliary extracellular vesicle biogenesis. Mol. Biol. Cell *26*, 2823–2832.
21. Hurd, D.D., Miller, R.M., Núñez, L., and Portman, D.S. (2010). Specific alpha- and beta-tubulin isotypes optimize the functions of sensory Cilia in Caenorhabditis elegans. Genetics *185*, 883–896.
22. Kaletsky, R., Lakhina, V., Arey, R., Williams, A., Landis, J., Ashraf, J., and Murphy, C.T. (2015). The C. elegans adult neuronal IIS/FOXO transcriptome reveals adult phenotype regulators. Nature. http://dx.doi.org/10.1038/nature16483.
23. Peden, E.M., and Barr, M.M. (2005). The KLP-6 kinesin is required for male mating behaviors and polycystin localization in Caenorhabditis elegans. Curr. Biol. *15*, 394–404.
24. Xie, P. (2013). TRAF molecules in cell signaling and in human diseases. J. Mol. Signal. *8*, 7.
25. Ewbank, J.J. (2006). Signaling in the immune response. WormBook, 1–12.
26. Li, C.J., Liu, Y., Chen, Y., Yu, D., Williams, K.J., and Liu, M.L. (2013). Novel proteolytic microvesicles released from human macrophages after exposure to tobacco smoke. Am. J. Pathol. *182*, 1552–1562.
27. Curtis, A.M., Wilkinson, P.F., Gui, M., Gales, T.L., Hu, E., and Edelberg, J.M. (2009). p38 mitogen-activated protein kinase targets the production of proinflammatory endothelial microparticles. J. Thromb. Haemost. *7*, 701–709.

28. Bianco, F., Perrotta, C., Novellino, L., Francolini, M., Riganti, L., Menna, E., Saglietti, L., Schuchman, E.H., Furlan, R., Clementi, E., et al. (2009). Acid sphingomyelinase activity triggers microparticle release from glial cells. EMBO J. *28*, 1043–1054.

29. Schroeder, N.E., Androwski, R.J., Rashid, A., Lee, H., Lee, J., and Barr, M.M. (2013). Dauer-specific dendrite arborization in C. elegans is regulated by KPC-1/Furin. Curr. Biol. *23*, 1527–1535.

30. Venancio, T.M., and Aravind, L. (2010). CYSTM, a novel cysteine-rich transmembrane module with a role in stress tolerance across eukaryotes. Bioinformatics *26*, 149–152.

31. Hiemstra, T.F., Charles, P.D., Gracia, T., Hester, S.S., Gatto, L., Al-Lamki, R., Floto, R.A., Su, Y., Skepper, J.N., Lilley, K.S., and Karet Frankl, F.E. (2014). Human urinary exosomes as innate immune effectors. J. Am. Soc. Nephrol. *25*, 2017–2027.

32. Maures, T.J., Booth, L.N., Benayoun, B.A., Izrayelit, Y., Schroeder, F.C., and Brunet, A. (2014). Males shorten the life span of C. elegans hermaphrodites via secreted compounds. Science *343*, 541–544.

33. Buck, A.H., Coakley, G., Simbari, F., McSorley, H.J., Quintana, J.F., Le Bihan, T., Kumar, S., Abreu-Goodger, C., Lear, M., Harcus, Y., et al. (2014). Exosomes secreted by nematode parasites transfer small RNAs to mammalian cells and modulate innate immunity. Nat. Commun. *5*, 5488.

34. Vader, P., Breakefield, X.O., and Wood, M.J. (2014). Extracellular vesicles: emerging targets for cancer therapy. Trends Mol. Med. *20*, 385–393.

Current Biology

Supplemental Information

Cell-Specific Transcriptional Profiling of Ciliated Sensory Neurons Reveals Regulators of Behavior and Extracellular Vesicle Biogenesis

Juan Wang, Rachel Kaletsky, Malan Silva, April Williams, Leonard A. Haas, Rebecca J. Androwski, Jessica N. Landis, Cory Patrick, Alina Rashid, Dianaliz Santiago-Martinez, Maria Gravato-Nobre, Jonathan Hodgkin, David H. Hall, Coleen T. Murphy, and Maureen M. Barr

Figure S1

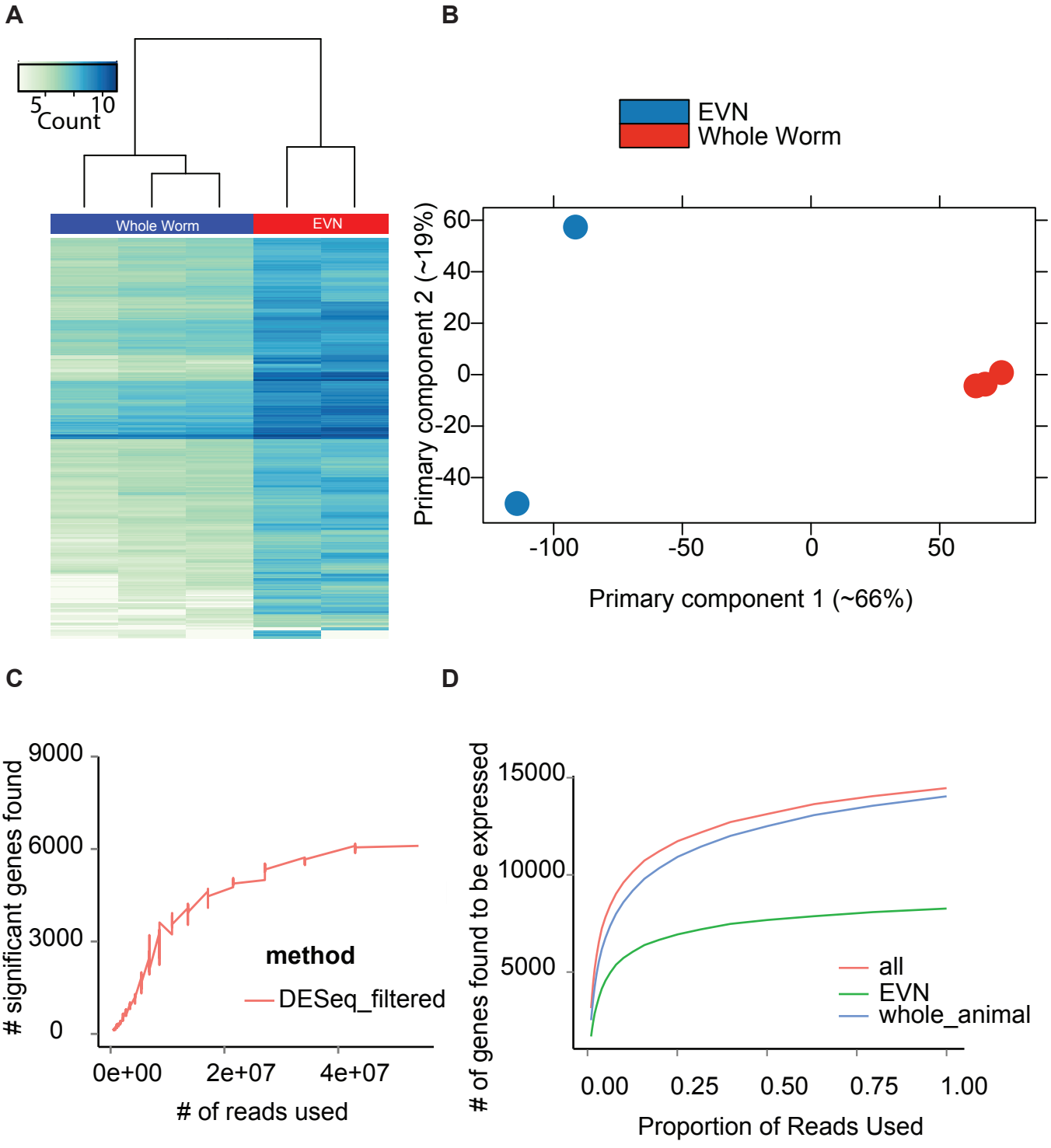
A
5
10
Count
Whole Worm
EVN
B
EVN
Whole Worm
Primary component 2 (~19%)
60
40
20
0
-20
-40
-100
-50
0
50
Primary component 1 (~66%)
C
significant genes found
9000
6000
3000
0
method
DESeq_filtered
0e+00
2e+07
4e+07
# of reads used
D
# of genes found to be expressed
15000
10000
5000
all
EVN
whole_animal
0.00
0.25
0.50
0.75
1.00
Proportion of Reads Used

Legends

Supplemental Figure 1, related to Figure 1C-E. (A) Heat map of all 14,464 genes found to be transcribed (>10 reads in at least one of all replicates) in either the whole worm lysates or sorted EVNs. (B) Principal component analysis (PCA) was performed on the normalized, variance stabilization transformed count data using DESeq. The variability captured by the first two principal components (~66% and ~19%) is shown. Isolated EVNs are more variable than the whole worm samples, the main principle component separates the two classes of samples nicely and explains most of the variation in the data. (C) Total reads were downsampled in silico [S1] to the reported proportions ten times and tested for differential expression as described in the text, number of genes found to be significantly differentially expressed (pad < 0.10) are reported on the y-axis. (D) Total reads were downsampled in silico to the reported proportions and tested for expression as described in the text (1/2 of all replicates have > 10 reads), number of genes found to be expressed according to this threshold are reported on the y-axis. From the downsampling, we can see that the number of DEGs we find is mostly saturated even at the depth we're using, not still in the exponential growth phase. There are only 20,000 genes in all of *C. elegans*, so it is not unexpected to detect 70% of these expressed in adult animals. Our data is also consistent with the proportions of whole transcriptome expressed in other more complex animals (mice, humans, etc.)

Table S1, related to Figure 1C-E, Figure 2. The 335 EVN signature genes. Expression pattern were validated by GFP reporter herein (Methods) or in cited publications. Genes that are exclusively expressed in EVNs are in bold. Genes that are expressed in EVNs and other cell types are underlined in bold. No expression indicates our GFP reporter transgenic lines showed no clear expression pattern. Not examined indicates the candidate has not been validated by GFP reporters in this study or other publications.

Table S2, related to Figure 1C-E. Original DEseq data for the differential RNAseq NA, not

available. Table has normalized counts. Per the method of Anders and Huber [S2], transcript count data are normalized, and size factor is calculated to allow the raw count data to then be compared.

Table S3, related to Figure 1. GO Analysis of EVN overrepresented genes. Citations for the programs used are: for GO analysis [S3]; for topGO (topGO: Enrichment analysis for Gene Ontology. R package version 2.22.0.), and the worm annotation package (Carlson M. org.Ce.eg.db: Genome wide annotation for Worm. R package version 3.2.3.). The latter was updated on Oct. 13, 2015. The GO terms are no longer enrichment clusters but are now just the terms unclustered, We used all three annotations (molecular function, biological process, and cell cycle).

Table S4, related to Figure 2, Figure 3, Figure 4 . Several EVN signature genes have predicted or demonstrated function in stress response or innate immunity.

Table S5, related to Figures 3 and 4. Response efficiency (RE) and location efficiency (LE) of mutants corresponding to new EVN signature genes and pathways. n= number of males assayed. Statistical analysis was done by Fisher's exact test, Bonferroni-Holm corrected for RE and one-way ANOVA for LE. Underlined cells are significantly different than wild type (p value indicated in parentheses).

Table S4 Putative immune genes and stress response genes in the EVN signature genes.

Class/gene name	rank	Log2 (klp6*p*::GFP sorted/unsorted)	P value	Ref
TRAF homologues				
trf-1	29	8.4	<0.001	[S4, S5]
trf-2	30	8.4	<0.001	[S5]
Transcription factors				
daf-19	264	3.3	0.011	[S5]
zip-2	275	3.2	0.011	[S6]
Signaling				
pmk-1	253	3.5	0.029	[S7]
jnk-1	260	3.4	0.038	[S8]
dgk-1	270	3.3	0.040	[S9]
F25B4.2	292	2.9	0.039	[S10]
Detoxifying				
gst-37	32	7.8	<0.001	[S11]
bre-2	106	6.3	0.004	[S12]
gst-28	190	4.3	0.008	[S11]
Stress resistance				
glb-28	74	7.8	0.017	[S13]
pme-4	90	6.9	0.025	[S14]
kin-29	295	2.8	0.023	[S15]
Antimicrobial peptides (AMP)				
F14D7.11	5	10.1	<0.001	[S16, S17]
Y26D4A.5	16	9.3	<0.001	[S16, S17]
F14D7.12	33	7.7	0	[S16, S17]
nlp-1	45	6.5	<0.001	[S18]
F02E11.2	69	8.6	0.047	[S16, S17]
F08G12.8	88	7	0.004	[S16, S17]
Y17G9B.11	128	5.6	0.04	[S16, S17]
R02E12.5	137	5.3	0.028	[S16, S17]
C44B11.4	159	4.8	0.042	[S16, S17]
T23F2.3	196	4.2	0.009	[S16, S17]
fipr-1	203	4.1	0.021	[S19]
K07D4.9	204	4.1	0.019	[S16, S17]
F09E5.16	221	3.9	0.044	[S16, S17]
C type lectin				
clec-179	8	9.8	<0.001	[S20]
clec-164	12	9.5	<0.001	[S20]
clec-113	38	7.4	0.001	[S20]

clec-254	59	Inf	0.002	[S20]
clec-256	62	Inf	0.011	[S20]
clec-255	64	9.3	0.028	[S20]
clec-188	67	9.1	0.015	[S20]
clec-176	75	8.2	0.002	[S20]
clec-251	78	7.8	0.001	[S20]
clec-114	104	6.4	0.002	[S20]
clec-194	105	6.4	0.002	[S20]
clec-112	109	6.3	0.005	[S20]
clec-250	201	4.1	0.045	[S20]
Galectin				
lec-9	292	2.7	0.047	[S20]
MIP-T3 domain				
M01A8.2	274	3.2	0.016	[S21]
S/T rich Mucin like domain				
C35A11.3	2	10.6	<0.001	[S22]
F26C11.3	4	10.3	<0.001	[S22]
F59A6.3	10	9.8	<0.001	[S22]
F49C5.7	21	8.8	<0.001	[S22]
Y53G8AL.3	66	9.2	0.001	[S22]
ZC204.6	83	7.5	0.013	[S22]

Bold genes were validated by GFP reporters that are exclusively expressed in EVNs (Figures 2, 3).

Supplemental Table 5. Mating behavior of candidate gene mutants.

Genotype	Encoding protein Domains/homology	RE (%)(n)	LE (%)(n)
wild type		98.4 ± 2.8 (184)	88.6 ± 1.7 (168)
pkd-2(sy606)	TRPP	15.2 ± 2.2(264)	27.4 ± 3.1 (10)
asic-2 (ok289)	DEG/ENaC	93.3 ± 2.9 (75)	81.8 ± 3.0 (66)
clec-164 (gk335531)	C-Lectin	96.0 ± 2.8 (50)	82.9 ± 3.5 (42)
egas-1 (ok3497)	DEG/ENaC	97.8 ± 1.6 (90)	72.5 ± 3.4 (82)
F26C11.3 ***(gk453581)***	CCP+Mucin like	76.7 ± 6.5 (43)	*54.9 ± 8.3 (16) (* p<0.001)*
F28A12.3(*tm6038)*	TGFβ receptor	96.6 ± 2.4 (59)	79.9 ± 3.9 (49)
F31F7.2(*WBVar00272087)*	vWA	94.6 ± 3.8 (37)	*61.8 ± 4.4 (35) (* p<0.001)*
F59A6.3(*gk643207)*	C-Lectin	100 ± 0 (25)	*54.9 ± 6.2 (25) (* p<0.001)*
nsy-1 (ok593)	MAPKKK	83.9 ± 6.7 (31)	88.7 ± 4.9 (28)
sek-1 (km4)	MAPKK	93.5 ± 3.7 (46)	86.5 ± 4.6 (43)
tir-1(tm3036)	TIR domain adaptor	85.4 ± 5.6 (41)	75.2 ± 6.3 (36)
F25D7.5*(tm4326);pkd-2(sy606)*	C-Lectin+5TM	14.6 ± 5.6 (41)	50.0 ± 18.0 (4)
Y70G10A.2*(gk183679)*	C-Lectin+5TM	97.5 ± 2.5 (40)	84.6 ±4.9 (39)

* Statistically different from wild type. F25D7.5*(tm4326);pkd-2(sy606) is statistically different from wild type but not pkd-2(sy606)*

Supplemental Experimental Procedures

***C. elegans* maintenance**

All nematodes were grown under standard conditions [S23]. The strain PT2519: *myIs13 [P_{klp-6}::gfp + pBX (plasmid pha-1(+)]; him-5(e1490) V* was used for adult cell isolation.

Adult EVN isolation was performed as described by [S24]. The integrated transgene *myIs13[P_{klp-6}::gfp + pBX]* was used to mark EVNs; the *him-5 (e1490)* mutation was used to generate a male enriched population. Eggs were collected by bleaching adult worms and plated on to HGM (High Growth Media; Same as NGM, except Bacto-peptone 20 g/L, cholesterol 20 mg/L, agar 30 g/L) plates to produce synchronized male-enriched worm cultures. Three plates of synchronized worms on HGM plates were used for each cell sorting. Worms were washed off of plates with M9 buffer (42 mM Na_2HPO_4, 22 mM KH_2PO_4, 86 mM NaCl, 1 mM $MgSO_4.7H_2O$), put into 1.5ml centrifuge tubes, and washed five more times in M9, until all of the bacterial food was removed. All centrifugation steps were performed in a standard mini-centrifuge (Fisher, max speed: 6000 rpm) for 5 seconds. The worms were then washed once in 500 µl lysis buffer (200 mM DTT, 0.25% SDS, 20 mM HEPES pH 8.0, 3% sucrose) at room temperature (RT). 750ul lysis buffer was added to each tube; animals were incubated at room temperature for exactly 6.5 min. The worms were again washed five times in M9 buffer and spun down. Then, 250 ul of freshly made Pronase (20 mg/mL in ddH20; from *Streptomyces griseus;* Sigma-Aldrich Cat No: P6911-1G) was added, and the worm pellet was incubated for 20 min at RT. The worm solution was pipetted vigorously with a P200 tip for 100 times every 5 min to release EVNs; a 2µl sample of worms was examined on a dissecting scope after every pipetting stage to assess the level of dissociation. PBS solution with 2% FBS (Fetal Bovine Serum, Certified, Heat-Inactivated, Invitrogen Cat No: 10082-139) was used to pre-wet a 5 µm syringe filter, which was stored on ice. The dissociated cells were taken up into a 1 mL syringe through a 27 gauge needle before fitting the cooled filter onto the syringe to gently filter cells into a FACS tube on ice. 1 mL PBS solution was used to wash the filter again to recover any remaining cells. The cells then were kept on ice and in darkness until sorting. Cells were sorted using FACSVantage SE w/DiVa (BD Biosciences) directly into 850ul Trizol LS; 150ul sorted cells were added (about

250,000 cells maximum) per tube. Unfiltered cells were used for whole worm cell RNAseq controls.

RNAseq

RNA isolation was according to the protocol for linear amplification microarrays [S25]. RNA-seq, computational analysis and significant gene list generation and transcript identification and abundance analysis (DEseq) was performed as described in [S24]. In brief total reads were downsampled in silico to the reported proportions and tested for expression and differential expression as described in the text. Refer also to Supplemental Figure 1 legend.

GFP reporter construction and transgenic worm generation: Promoter and translational GFP reporters were created using the PCR fusion technique [S26]. A promoter region is chosen according to the following criteria: if intergenic region upstream of start codon is larger than 2 Kb, then 2 Kb sequence upstream of start codon of the gene was used; if the intergenic region upstream of the start codon is smaller than 2 Kb, the whole intergenic region upstream of the start codon was used. For all translational reporters, promoter plus the genomic coding region was fused to GFP coding sequence. 200 ng/µL PCR product of reporter were mixed with 50 ng/µl of pBX and injected into PS2172: *pha-1(e1213ts)III; him-5(e1490)V.*

Mating behavior assays: Response and vulva location assays were modified from [S27]. Briefly, a mating assay lawn was prepared by dropping 13 µl of OP50 *Escherichia coli* bacterial culture in LB broth onto a fresh NGM plate and allowed to dry covered overnight, making a circular lawn of ~ 0.5 cm diameter. Ten minutes prior to the assay, 20 hermaphrodites were scattered onto the mating dot and allowed to acclimate. Male mating behavior was assayed blind as follows: 5 males of the first genotype were released in the center of the mating lawn and observed for 4 minute time period. Response was scored positive when a male touched a hermaphrodite with its tail and began backward scanning of the hermaphrodite. Location of vulva efficiency was

scored by 1 divided by the number of times a male contacted the hermaphrodite vulva until stopping at the vulva. Leaving assays are described in [S28]. Each male genotype was assayed at least three times on separate days to compensate for behavioral variability and to ensure robustness of the results. CB1490: *him-5(e1490)V* males were used as positive wild-type controls, and PT9: *pkd-2(sy606)IV; him-5(e1490)V* males were used as negative controls.

EV release quantification and imaging: Strain PT621 *him-5(e1490) myIs4 [PKD-2::GFP +$P_{unc-122}$::gfp]V* was used as wild type. Both late L4 males and adult males were examined for EV release according to [S29]. Worms were imaged using a Zeiss Axioplan 2 microscope with a 100x 1.4NA oil Zeiss Plan-APOCHROMA objective and Photometrics Cascade 512B EMCCD (Roper Scientific) camera or Zeiss 510 laser scanning confocal microscope. Young adult males were synchronized by picking L4 larvae one day before imaging. Late L4 males with developed fan and rays just before molting were picked from a population of L4 males and imaged within 1-5 hours. Worms were anesthetized with 10 mM levamisole solution, transferred to 2% agarose mounting slides and imaged within 30 minutes of mounting.

Transmission electron microscopy

Young adult nematodes were prepared by high pressure freezing and freeze substitution following described protocols described [S30]. Principal fixation involved 1% osmium, 3% dH2O in acetone. Serial thick sections were collected onto Pioloform-coated slot grids and examined using a Technai F20 electron microscope. Serial section dual axis electron tomograms were produced from consecutive semi-thick sections (200 nm) using markerless alignment and internal back projection methods, followed by mergers of electron tomograms from consecutive sections [S31].

Strain list

Strain	Genotype	REF
CB1490	*him-5(e1490)V*	[S32]
PT9	*pkd-2(sy606)IV; him-5(e1490)V*	[S33]
PT2915	*pmk-1(km25)IV; him-5(e1490), myIs4(PKD-2::GFP+unc-122p::GFP)V*	This study
PT2951	*pmk-1(km25)IV; him-5(e1490)V*	This study
PT621	*him-5(e1490), myIs4V*	[S34]
PT2946	*tir-1(tm3036) III; him-5(e1490)V; myIs1(PKD-2::GFP+unc-122p::GFP)IV*	This study
PT2947	*nsy-1(ok593) II; him-5(e1490)V; myIs1*	This study
PT2948	*him-5(e1490)V; sek-1(km4) X; myIs1*	This study
PT2949	*nsy-1(ok593) II; him-5(e1490)V*	This study
PT2950	*him-5(e1490)V; sek-1(km4) X*	This study
PT2376	*trf-1(nr2014)III;him-5(e1490)V*	This study

PT2393	*trf-1(nr2014), pha-1(e2123)III; him-5(e1490)V; myEx750 (TRF-1::GFP+*	This study
PT1722	*pha-1(e2123) III; him-5(e1490) V; myEx632[Pklp-6::tdTomato + pBX1]*	This study
PT2395	*pha-1(e2123)III; him-5(e1490)V; myEx750, myEx632*	This study
PT9	*pkd-2 (sy606)IV;him-5(e1490)V*	This study
PS3401	*lov-1(sy582)II;him-5(e1490)V*	[S27]
PT2411	*trf-1(nr2014)III;pkd-2(sy606)IV;him-5(e1490)V*	This study
PT2412	*lov-1(sy582)II;trf-1(nr2014)III;him-5(e1490)V*	This study
PT2413	*lov-1(sy582)II;trf-1(nr2014)III;pkd-2(sy606)IV;him-5(e1490)V*	This study
PT2414	*tol-1(nr2033)I;him-5(e1490)V*	This study
PT2415	*ikb-1(nr2027)I;him-5(e1490)V*	This study
PT443	*pkd-2(sy606)VI;him-5(e1490);myIs1*	This study
PT2394	*trf-1(nr2014)III;pkd-2(sy606)VI;him-5(e1490);myIs1*	This study
PT2864	*pha-1(e2123) III; him-5(e1490) V; myEx865[GLB-28::GFP+ pBX1]*	This study
PT2882	*pha-1(e2123) III; him-5(e1490)V; myEx869[F26C11.3::GFP+ pBX1]*	This study
PT2753	*pha-1(e2123) III; him-5(e1490) V; myEx841[C35A11.3p:GFP)+pBX1]*	This study
PT2945	*pha-1(e2123) III; him-5(e1490) V; myEx877[F25D7.5::GFP+pBX1]*	This study
PT2871	*pha-1(e2123) III; him-5(e1490) V; myEx858[T09D9.3::GFP+pBX1]*	This study
PT2879	*pha-1(e2123) III; him-5(e1490) V; myEx866[TF49C5.12::GFP+pBX1]*	This study
PT2461	*him-5(e1490)V; myEx732[F28A12.3p::GFP,elt-2::mCherry]*	This study
PT2862	*pha-1(e2123) III; him-5(e1490) V;myEx855[T13F3.7p::G)+Pklp-6::tdTomato*	This study
PT2872	*pha-1(e2123) III; him-5(e1490) V; myEx859[C18F10.2::GFP+pBX1]*	This study
PT2859	*pha-1(e2123) III; him-5(e1490) V; myEx859[C18F10.2::GFP+pBX1]*	This study
PT2889	*pha-1(e2123) III; him-5(e1490) V; myEx874[T06D8.2::GFP+pBX1]*	This study
PT2971	*pha-1(e2123) III; him-5(e1490) V; myEx876[F14D7.11::GFP+pBX1]*	This study
PT2751	*pha-1(e2123) III; him-5(e1490) V; myEx839[egas-1p::GFP+pBX1]*	This study

PT2757	*pha-1(e2123) III; him-5(e1490) V; myEx845[F59A6.3::GFP+pBX1]*	This study
PT2860	*pha-1(e2123) III; him-5(e1490) V;myEx853[Y70G10A.2::GFP+pBX1]*	This study
PT2564	*pha-1(e2123) III; him-5(e1490) V; myEx840[ASIC-2::GFP+ pBX1]*	This study
PT2875	*pha-1(e2123) III; him-5(e1490) V; myEx862[CLEC-164::GFP+pBX1]*	This study
PT2944	*pha-1(e2123) III; him-5(e1490) V; myEx878[clec-179p::GFP+pBX1]*	This study
PT2901	*clec-164(gk335531) IV; him-5(e1490) V*	This study
PT2902	*clec-164(gk335531) IV; him-5(e1490), myIs4 V*	This study
PT2894	*F25D7.5(tm4326)I; pkd-2(sy606)IV; him-5(e1490)V*	This study
PT2895	*F25D7.5(tm4326)I; pkd-2(sy606), myIs1IV; him-5(e1490)V*	This study
PT2912	*F59A6.3(gk643207)II; pkd-2(sy606), myIs1IV; him-5(e1490)V*	This study
PT2913	*F59A6.3(gk643207)II; him-5(e1490)V*	This study
PT2914	*F26C11.3(gk453581)II; him-5(e1490)V*	This study
PT2900	*F26C11.3(gk453581)II; pkd-2(sy606), myIs1IV; him-5(e1490)V*	This study
PT2761	*asic-2(ok289) I; myIs13[klp-6p::GFP + pBX1] III; him-5(e1490) V*	This study
PT2898	*Y70G10A.2(gk183679)III; him-5(e1490)V*	This study
PT2899	*Y70G10A.2(gk183679)III; pkd-2(sy606), myIs1IV; him-5(e1490)V*	This study
PT2732	*pkd-2(sy606),him-8(e1489)IV, myIs1; egas-1(ok3497)V*	This study
PT2867	*myIs13III; egas-1(ok3497)V*	This study

Supplemental References

S1. Robinson, D.G., and Storey, J.D. (2014). subSeq: determining appropriate sequencing depth through efficient read subsampling. Bioinformatics *30*, 3424-3426.

S2. Anders, S., and Huber, W. (2010). Differential expression analysis for sequence count data. Genome Biol *11*, R106.

S3. Alexa, A., Rahnenfuhrer, J., and Lengauer, T. (2006). Improved scoring of functional groups from gene expression data by decorrelating GO graph structure. Bioinformatics *22*, 1600-1607.

S4. Pujol, N., Bonnerot, C., Ewbank, J.J., Kohara, Y., and Thierry-Mieg, D. (2001). The Caenorhabditis elegans unc-32 gene encodes alternative forms of a vacuolar ATPase a subunit. J Biol Chem *276*, 11913-11921.

S5. Xie, P. (2013). TRAF molecules in cell signaling and in human diseases. J Mol Signal *8*, 7.

S6. Estes, K.A., Dunbar, T.L., Powell, J.R., Ausubel, F.M., and Troemel, E.R. (2010). bZIP transcription factor zip-2 mediates an early response to Pseudomonas aeruginosa infection in Caenorhabditis elegans. Proc Natl Acad Sci U S A *107*, 2153-2158.

S7. Aballay, A., Drenkard, E., Hilbun, L.R., and Ausubel, F.M. (2003). Caenorhabditis elegans Innate Immune Response Triggered by Salmonella enterica Requires Intact LPS and Is Mediated by a MAPK Signaling Pathway. Curr Biol *13*, 47-52.

S8. Oh, S.W., Mukhopadhyay, A., Svrzikapa, N., Jiang, F., Davis, R.J., and Tissenbaum, H.A. (2005). JNK regulates lifespan in Caenorhabditis elegans by modulating nuclear translocation of forkhead transcription factor/DAF-16. Proc Natl Acad Sci U S A *102*, 4494-4499.

S9. Kao, C.Y., Los, F.C., and Aroian, R.V. (2008). Nervous about immunity: neuronal signals control innate immune system. Nat Immunol *9*, 1329-1330.

S10. Nicholas, H.R., and Hodgkin, J. (2004). Responses to infection and possible recognition strategies in the innate immune system of Caenorhabditis elegans. Mol Immunol *41*, 479-493.

S11. Hasegawa, K., Miwa, S., Isomura, K., Tsutsumiuchi, K., Taniguchi, H., and Miwa, J. (2008). Acrylamide-responsive genes in the nematode Caenorhabditis elegans. Toxicol Sci *101*, 215-225.

S12. Marroquin, L.D., Elyassnia, D., Griffitts, J.S., Feitelson, J.S., and Aroian, R.V. (2000). Bacillus thuringiensis (Bt) toxin susceptibility and isolation of resistance mutants in the nematode Caenorhabditis elegans. Genetics *155*, 1693-1699.

S13. Tilleman, L., Germani, F., De Henau, S., Geuens, E., Hoogewijs, D., Braeckman, B.P., Vanfleteren, J.R., Moens, L., and Dewilde, S. (2011). Globins in Caenorhabditis elegans. IUBMB Life *63*, 166-174.

S14. St-Laurent, J.F., Gagnon, S.N., Dequen, F., Hardy, I., and Desnoyers, S. (2007). Altered DNA damage response in Caenorhabditis elegans with impaired poly(ADP-ribose) glycohydrolases genes expression. DNA Repair (Amst) *6*, 329-343.

S15. Lanjuin, A., and Sengupta, P. (2002). Regulation of chemosensory receptor expression and sensory signaling by the KIN-29 Ser/Thr kinase. Neuron *33*, 369-381.

S16. Thomas, S., Karnik, S., Barai, R.S., Jayaraman, V.K., and Idicula-Thomas, S. (2010). CAMP: a useful resource for research on antimicrobial peptides. Nucleic Acids Res *38*, D774-780.

S17. Waghu, F.H., Gopi, L., Barai, R.S., Ramteke, P., Nizami, B., and Idicula-Thomas, S. (2014). CAMP: Collection of sequences and structures of antimicrobial peptides. Nucleic Acids Res *42*, D1154-1158.
S18. Ren, M., Feng, H., Fu, Y., Land, M., and Rubin, C.S. (2009). Protein kinase D is an essential regulator of C. elegans innate immunity. Immunity *30*, 521-532.
S19. Pujol, N., Davis, P.A., and Ewbank, J.J. (2012). The Origin and Function of Anti-Fungal Peptides in C. elegans: Open Questions. Front Immunol *3*, 237.
S20. Schulenburg, H., Hoeppner, M.P., Weiner, J., 3rd, and Bornberg-Bauer, E. (2008). Specificity of the innate immune system and diversity of C-type lectin domain (CTLD) proteins in the nematode Caenorhabditis elegans. Immunobiology *213*, 237-250.
S21. Ling, L., and Goeddel, D.V. (2000). MIP-T3, a novel protein linking tumor necrosis factor receptor-associated factor 3 to the microtubule network. J Biol Chem *275*, 23852-23860.
S22. Lieleg, O., Lieleg, C., Bloom, J., Buck, C.B., and Ribbeck, K. (2012). Mucin biopolymers as broad-spectrum antiviral agents. Biomacromolecules *13*, 1724-1732.
S23. Brenner, S. (1974). The genetics of Caenorhabditis elegans. Genetics *77*, 71-94.
S24. Kaletsky, R., Williams, A.B., Arey, R., Lakhina, V., Landis, J.L., and Murphy, C.T. (in review). Transcriptional profiling of isolated adult C. elegans neurons identifies the neuronal IIS/FOXO transcriptome and a new regulator of axon regeneration.
S25. Murphy, C.T., McCarroll, S.A., Bargmann, C.I., Fraser, A., Kamath, R.S., Ahringer, J., Li, H., and Kenyon, C. (2003). Genes that act downstream of DAF-16 to influence the lifespan of Caenorhabditis elegans. Nature *424*, 277-283.
S26. Hobert, O. (2002). PCR fusion-based approach to create reporter gene constructs for expression analysis in transgenic C. elegans. Biotechniques *32*, 728-730.
S27. Barr, M.M., and Sternberg, P.W. (1999). A polycystic kidney-disease gene homologue required for male mating behaviour in C. elegans. Nature *401*, 386-389.
S28. Lipton, J., Kleemann, G., Ghosh, R., Lints, R., and Emmons, S.W. (2004). Mate searching in Caenorhabditis elegans: a genetic model for sex drive in a simple invertebrate. J Neurosci *24*, 7427-7434.
S29. Wang, J., Silva, M., Haas, L.A., Morsci, N.S., Nguyen, K.C., Hall, D.H., and Barr, M.M. (2014). C. elegans Ciliated Sensory Neurons Release Extracellular Vesicles that Function in Animal Communication. Curr Biol *24*, 519-525.
S30. Hall, D.H., Hartwieg, E., and Nguyen, K.C. (2012). Modern electron microscopy methods for C. elegans. Methods Cell Biol *107*, 93-149.
S31. Hall, D.H., and Rice, W.J. (2015). Electron tomography methods for C. elegans. In C. elegans, Methods and Applications, Volume in press, G. Haspel and D. Biron, eds. (Humana Press).
S32. Hodgkin, J. (1983). Male phenotypes and mating efficiency in Caenorhabditis elegans. Geneitcs *103*, 43-64.
S33. Barr, M.M., DeModena, J., Braun, D., Nguyen, C.Q., Hall, D.H., and Sternberg, P.W. (2001). The Caenorhabditis elegans autosomal dominant polycystic kidney disease gene homologs lov-1 and pkd-2 act in the same pathway. Curr Biol *11*, 1341-1346.
S34. Bae, Y.K., Lyman-Gingerich, J., Barr, M.M., and Knobel, K.M. (2008). Identification of genes involved in the ciliary trafficking of *C. elegans* PKD-2. Dev Dyn *237*, 2021-2029.